STRUCTURAL DYNAMICS AND CONTROLS FOR NGST A PRELIMINARY STUDY

O. de Weck[1], D. Miller[2], H. Guiterrez[1]
Space Systems Laboratory
Department of Aeronautics and Astronautics
Massachusetts Institute of Technology
77 Massachusetts Avenue, Cambridge, MA 02139, U.S.A.
email: deweck@mit.edu
fax: (617) 258-5940

ABSTRACT

The Next Generation Space Telescope (NGST) poses a challenging problem from the point of view of controlled structures technology (CST). This is due to the extensive use of inflatable and deployable lightweight components (fundamental frequency at 0.3 Hz). This preliminary study carries out an initial disturbance to performance vibration analysis for the NGST optical telescope assembly (OTA). The opto-structural performance metrics used are the optical pathlength difference (OPD) and the wavefront tilt (WFT). The disturbance source is a Hubble-class reaction wheel assembly (RWA), which is described in the frequency domain by a 6x6 cross spectral density matrix. The results for the science observation mode (boresight aimed at a specific science target) indicate that the cumulative RMS values exceed the prescribed output levels for a wavelength of 0.5 μm. This suggests that, based on Hubble-like disturbances, the performance can only be met with structural redesign or active wavefront control. Time optimal slewing is of interest in the acquisition of new science targets. Input shaping of attitude control system (ACS) input commands is illustrated as a means of significantly decreasing the post-maneuver settling time. The preliminary results of this study are a basis for future work on integrated modeling of opto-structural problems for NGST.

Keywords: dynamics; vibration analysis; RWA; controlled structures technology; slewing; modeling; finite element models; optics performance.

1. INTRODUCTION

The Next Generation Space Telescope (NGST) is a challenging and interesting problem from the point of view of structural dynamics, optics and controlled structures technology (CST). This is due to the extensive use of inflatable and deployable lightweight components. An example is the flexible, inflatable sunshield which has a surface area of approximately 200 m^2 in the deployed configuration. It is this sunshield, which is responsible for the first flexible mode at a fundamental frequency of 0.301 Hz. Figure 1 shows a representation of the spacecraft configuration according to the NASA Goddard SFC concept [1], which was the basis for this work.

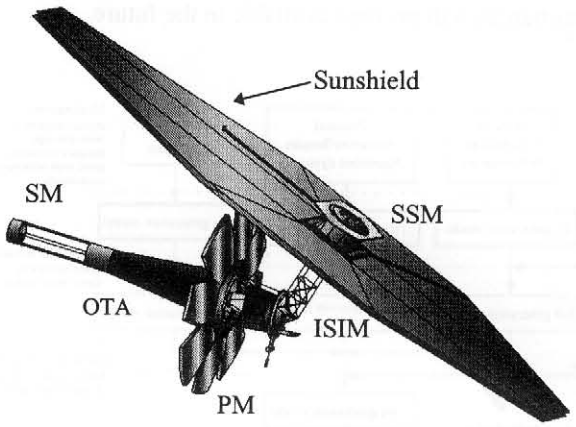

***Fig. 1** NGST configuration according to NASA GSFC (1996)*

NGST will be optimized for an observation wavelength of 1-5 μm, whereby the OTA shall be diffraction limited at 2.2 μm [2]. This requires that all components of the optical train, including the primary mirror (PM), the secondary mirror (SM), and the components inside the Integrated Science Instrument Module (ISIM) are aligned to within a fraction of wavelength. This is the reason why active vibration sensing and control have been previously identified as a key technology element for NGST [2].

This preliminary study focuses on the opto-structural performance metrics which describe the optical pathlength difference (OPD) and the wavefront tilt (WFT). It is assumed that the largest contributions to the OPD and WFT are due to the flexible motion of the primary mirror petals and the secondary mirror support structure. The objective is to perform a stochastic disturbance-to-performance analysis in order to determine whether the established performance metrics for the OTA can be met in the current configuration.

[1] Graduate Research Assistant, M.I.T. Space Systems Laboratory
[2] Assistant Professor, M.I.T. Space Systems Laboratory

Proceedings 34th Liège International Astrophysics Colloquium 'The Next Generation Space Telescope: Science Drivers and Technological Challenges', Liège, Belgium, 15-18 June 1998 (ESA SP-429, October 1998)

2. MODELING

The first step consists in building an opto-structural model of NGST and the OTA in particular. Due to the geometric complexity of the structure a finite element model (FEM) has been generated. The model employed here is based on a 5400 degree of freedom model, which was originally developed by GSFC/JPL. This model is a reduced FEM, whereby the original GSFC model contained 7500 dof. The sunshield, SSM and isolation truss are represented by simple beam and rod elements and point masses. The mass of the SMM is concentrated and an appropriate inertia matrix is assigned. Figure 2 shows that this model has to be considered as a 1st generation model within the controlled structures technology (CST) framework. A 2nd generation model will only be obtained, when experimental data on the actual or scaled structure, actuators, sensors and disturbances will become available in the future.

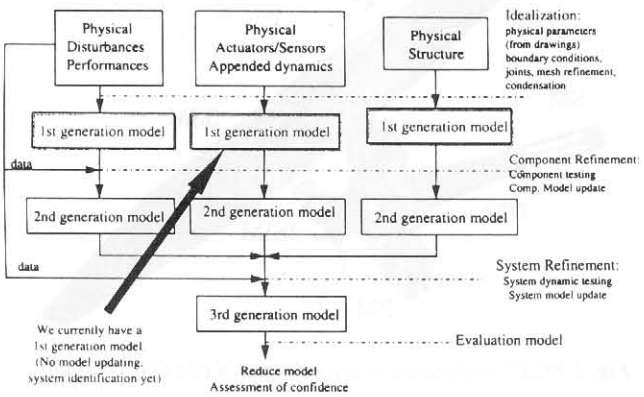

Fig.2 Classification of 1st generation model of NGST

The eigenfrequencies ω_i and modeshapes ϕ_i of this structure are obtained via a Normal Modes Analysis. The MSC/NASTRAN program with the Lanzcos eigensolver was used. The eigenfrequencies can also be represented via Rayleigh's equation:

$$\omega_i^2 = \frac{\{\phi_i\}^T [K] \{\phi_i\}}{\{\phi_i\}^T [M] \{\phi_i\}}$$

where K and M are the global stiffness and mass matrices respectively. The first 100 modes were obtained, whereby 6 rigid body modes of NGST are included. Figure 3 shows mode number 26 at 7.37 Hz as an example. This mode is interesting as it represents the first flexible mode, which involves global strain energy distribution including OTA pitch motion, secondary tower bending and higher order sunshield bending.

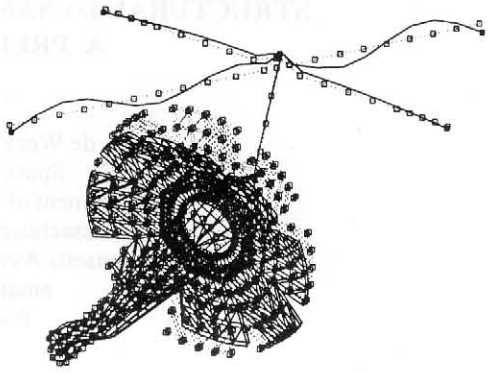

Fig.3 NGST flexible mode number 26 at 7.37 Hz

In order to verify the consistency of the results a comparison was made with modeshapes and eigenfrequencies obtained with the sparse eigensolver from IMOS [3]. It was determined that a very good match is obtained up to mode 32 as indicated in Figure 4. The modal assurance criterion (MAC) was used to verify the cross-orthogonality of modeshapes obtained from the MSC/NASTRAN (1) and IMOS (2) solvers respectively. A MAC value of 1.0 indicates a perfect match, whereby the MAC is defined as follows:

$$MAC_{ij} = \frac{\left|\phi_1(i)^T \cdot \phi_2(j)\right|}{\left|\phi_1(i)\right| \cdot \left|\phi_2(j)\right|}$$

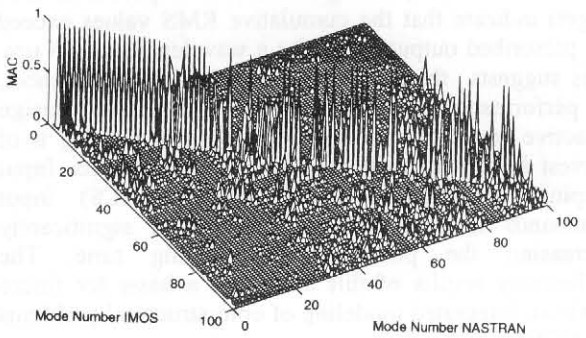

Fig.4 Modeshape Orthogonality MSC/NASTRAN vs. IMOS

A transformation to 2nd order modal form allows for a state space representation, where the states x of the dynamic system correspond to the modal coordinates of the structure. This state space system is the basis for the frequency-domain disturbance analysis, where w are the disturbances and z are the performances,

$$\dot{\underline{x}} = A\underline{x} + B_w \underline{w}$$
$$\underline{z} = C_z \underline{x} + D\underline{w}$$

It is in this orthonormal modal form that uniform modal damping of $\xi = 0.001$ was added to the system. There exists evidence from GSFC that the actual amount of damping is not uniform with frequency and that the "warm" and "cold" sections of the telescope will experience different amounts of structural damping as the

dissipative mechanisms in materials and joints are themselves temperature dependent. The C_z matrix contains the output influence coefficients, which describe the performances as a linear combination of the physical displacements of the structure.

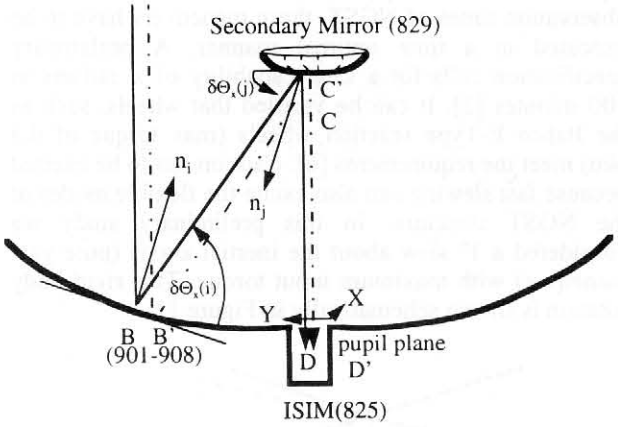

Fig.5 Representation of opto-structural performances

For a quantification of the wavefront error three different performance metrics were established. These are based on a geometric optics approach [4]. The optical path-length difference (OPD) is a measure for the phase difference of a ray, which is traced through the optical train from the primary mirror to the ISIM, compared to a ray in the unperturbed configuration. The wavefront tilt is the angle between the incident ray and the focal plane normal vector. In this study the wavefront tilt is determined in the x and y axes at the ISIM focal plane at the base of the secondary support tower (WFTX and WFTY). These performances are linearized and are shown schematically in Figure 5. Finally a transfer function matrix $G_{zw}(\omega)$ can be obtained, where we have 3 force and 3 moment inputs at the ACS input node of the finite element model and 24 outputs (one ray per primary mirror petal at nodes 901-908) in the preliminary study. Figure 6 shows a Bode plot for a representative transfer function from moment M_z at the ACS to the OPD for primary mirror petal 1.

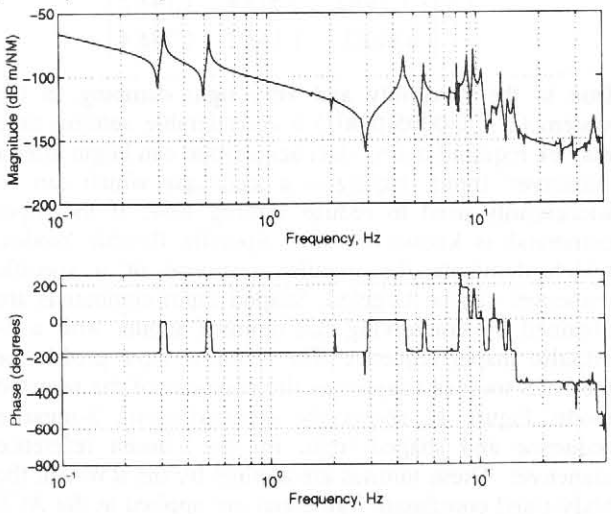

Fig.6 Transfer function from ACS M_z to OPD at PM petal 1

The transfer function matrix is evaluated in MATLAB at each frequency point and is a basis for the frequency domain disturbance analysis.

3. DISTURBANCE ANALYSIS

The disturbance analysis quantifies the effects of reaction wheel assembly (RWA) disturbances during science operations on the wavefront error. For this study a Hubble-class disturbance model according to Melody [5]. was assumed. The 4 reaction wheels in the assembly are assumed to be arranged in a pyramidal "equal torque" configuration. Each reaction wheel contributes to the power spectral densities (PSD) at the ACS point in the 3 spacecraft coordinate axes. Figure 7 shows the assumed pyramidal arrangement of the RWA.

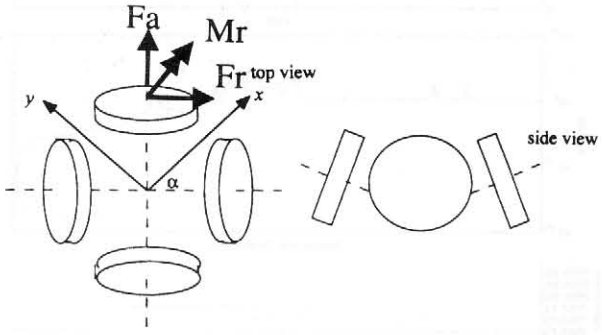

Fig. 7 Pyramidal arrangement in NGST RWA (4 wheels)

The disturbance PSD's for each wheel are contained in a 6x6 cross spectral density matrix $S_{mm}(\omega)$. To obtain the cross spectral density matrix of the total disturbance $S_{ww}(\omega)$ in spacecraft axes, the individual wheel PSD's have to be rotated into the spacecraft axes with the transformation matrix T_p and then summed together:

$$S_{ww}(\omega) = \sum_{p=1}^{\#wheels} T_p S_{mm}(\omega) T_p^T$$

The stochastic disturbance source is thus completely defined in the frequency domain. Figure 8 shows the PSD's for the preliminary RWA analysis. It can be seen that the spectral density functions roll off around 300 Hz.

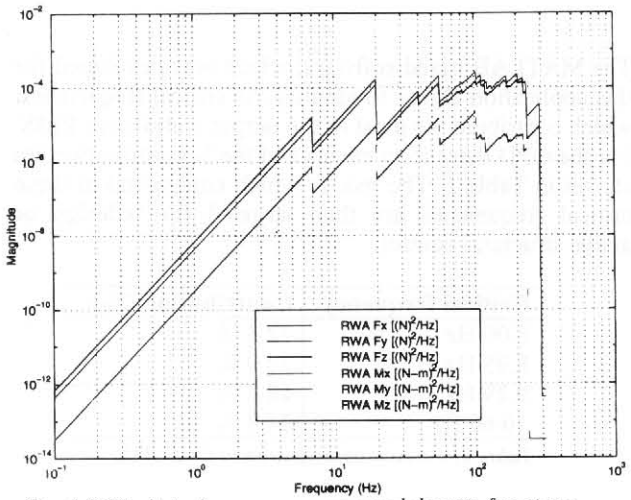

Fig. 8 RWA disturbance power spectral density functions

The frequency domain approach allows to propagate the disturbance PSD's in a very simple manner according to equation

$$S_{zz}(\omega) = G_{zw}(j\omega) \cdot S_{ww}(\omega) \cdot G_{zw}^{H}(j\omega)$$

where $G_{zw}(j\omega)$ is the transfer function matrix and $S_{ww}(\omega)$ is the disturbance cross spectral density matrix. The root mean square (RMS) value of the output can be obtained by integrating the output PSD's over all frequencies. Figure 10 shows a cumulative RMS plot for the OPD at the primary petal mirror 1 as an example.

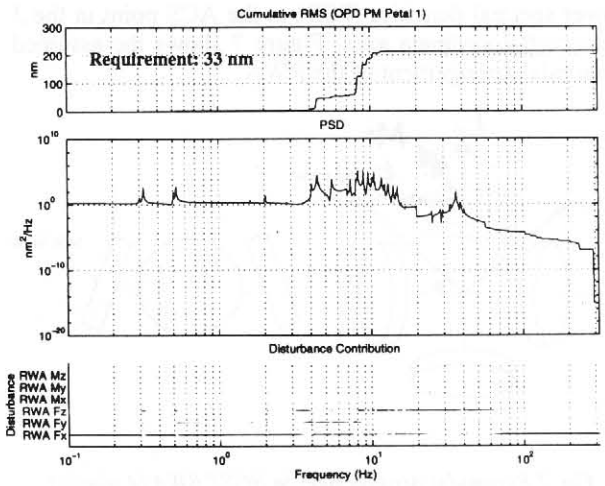

Fig.10 Resulting cumulative RMS of OPD at PM petal 1

For this particular ray the resulting performances, described by their output RMS values are summarized in Table 1. It can be seen that the vibration levels, which are induced by a Hubble-class reaction wheel exceed the specification levels.

Performance metric	Requirement	Actual value
OPD PM Petal 1:	33 nm	213 nm
WFTX PM Petal 1:	4.8 mas	25.7 mas
WFTY PM Petal 1:	4.8 mas	53.6 mas

***Table 1:** RMS values of outputs for OPD*

The MATLAB based software, which was developed for this application allows to identify the critical frequencies, which contribute the most to the output cumulative RMS. For the OPD these frequencies and the % contribution are shown in Table 2. The modes which correspond to these critical frequencies are then targeted for redesign or active structural control.

Critical frequency	Contribution (%)
8.00 Hz	22.3 %
8.95 Hz	22.9 %
9.29 Hz	12.3 %
10.66 Hz	14.4 %

***Table 2:** Percent contribution to OPD RMS*

4. TIME OPTIMAL SLEWING

Another important operational mode of NGST is the acquisition of new science targets. In order to precisely change the orientation of the spacecraft, the ACS issues input command torques. In order to maximize the observation times of NGST, these maneuvers have to be executed in a time optimal manner. A preliminary specification calls for a slew capability of π radians in 100 minutes [2]. It can be verified that wheels, such as the Itahco E-Type reaction wheels (max torque of 0.3 Nm) meet the requirements [6]. Caution has to be exerted because fast slewing can also excite the flexible modes of the NGST structure. In this preliminary study we considered a 1° slew about the inertial z-axis (pure yaw maneuver) with maximum input torque. This rigid body rotation is shown schematically in Figure 11.

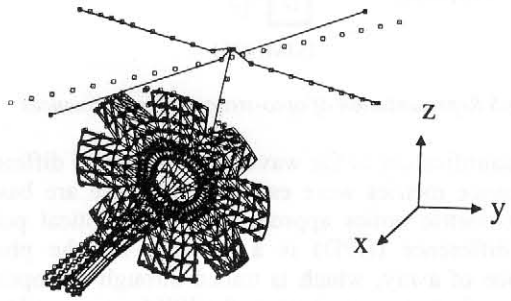

***Fig.11** Rigid body rotation about inertial z-axis (1°)*

For the derivation of the nominal input profiles we initially only consider rigid body motion. The instantaneous torques M and angular accelerations α are related via the body fixed inertia matrix:

$$\underline{M} = \frac{d\underline{\underline{H}}}{dt} = \underline{\underline{I}} \cdot \underline{\alpha}$$

From FEM analysis we obtain the inertia matrix (units: kgm^2) of NGST in body fixed axes as:

$$\underline{\underline{I}} = \begin{bmatrix} 1.22E4 & -1.36E2 & 6.86E3 \\ -1.36E2 & 2.51E4 & 1.14E2 \\ 6.86E3 & 1.14E2 & 1.78E4 \end{bmatrix}$$

Due to the flexibility and very light damping in the system (ξ = 0.0005-0.001) a considerable settling time may be required before data acquisition can begin after a maneuver. Input shaping is a technique which can be successfully used to reduce settling time, if the input command is known a-priori. Specific flexible modes, which dominate the impulse response of a specific maneuver can be targeted. Shaped input commands are obtained by convolving the nominal inputs with a 3-impulse shaper sequence. The resulting input profile for the ACS torques suppresses the response of the targeted mode. Figure 12 shows the nominal input, 3-impulse sequence and shaped input for the chosen reference maneuver. These torques are applied by the RWA in the body-fixed coordinate frame and are applied at the ACS input node (10291).

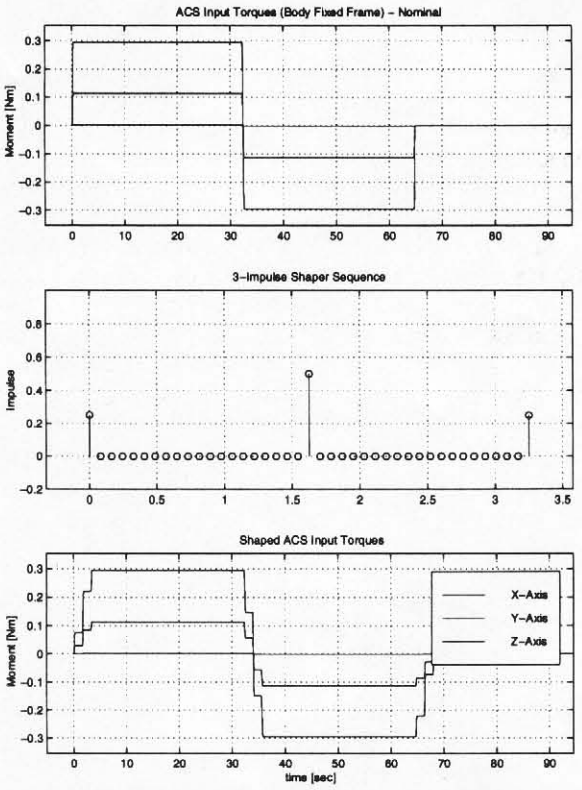

Fig.12 Nominal and shaped ACS input commands

The difference in the residual vibration levels after the maneuver can be significant. The settling time can be determined by calculating the a-posteriori OPD. The optical pathlength difference has to fall below the diffraction limit $\lambda/15$ before a new observation can begin. Figure 13 shows that the OPD for primary mirror (PM) petal #1 is out of tolerance during the slew maneuver (duration 65 sec) and immediately after the maneuver. It can be seen that larger residual vibration is present for the nominal inputs.

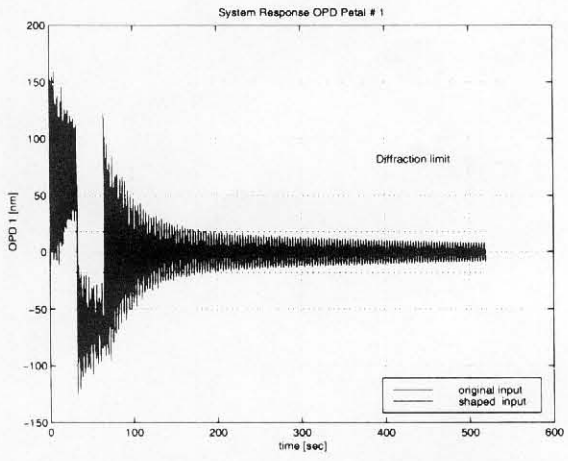

Fig.13 Settling time for NGST post-maneuver

Different flexible modes were targeted by the shaping filter. The largest improvement in settling time is obtained, when targeting the flexible sunshield mode at 0.526 Hz. The results of the input shaping study are summarized in Table 3. A small loss in rise time is traded with a significant improvement in settling time.

Mode #	Freq.	Settling time nominal	Settling time shaped
8	0.320 Hz	121.89 sec	39.98 sec
10	0.526 Hz	121.89 sec	23.15 sec
21	4.450 Hz	121.89 sec	108.11 sec

***Table 3**: Input shaping results summary*

5. CONCLUSIONS

The preliminary results indicate that the current configuration of NGST exhibits a low fundamental frequency and high modal density due to the use of deployable and low-areal density components. The RMS values of OPD and WFT are above the allowable levels for Hubble-based stochastic reaction wheel disturbances. It can also be concluded that the resonances in the region from 8-11 Hz contribute the most to the OPD cumulative RMS value. This suggests that a passive opto-structural redesign and/or active control will be necessary in order to insure compliance with the NGST technical requirements.

Future work will focus on developing NGST specific RWA disturbance input data, building OPD and WFT maps over all primary mirror nodes and conducting sensitivity analyses with respect to redesign options. Controls modeling will include the ACS, isolation truss and optics loops. Validation of the methodologies will be carried out with the help of M.I.T.'s ORIGINS precision telescope testbed.

ACKNOWLEDGMENTS

This research is supported by M.I.T. internal funds and by NASA's Goddard Space Flight Center in Greenbelt, MD under a RTOP research grant. Mr. Gary Mosier is providing technical monitoring and assistance. The help of Andy Kissil (JPL) in obtaining FEM data and resolving structural issues is gratefully acknowledged.

REFERENCES

[1] URL Source: http://ngst.gsfc.nasa.gov/

[2] NGST presentation to NGST study office, NASA Goddard Space Flight Center, August 21, 1996

[3] Integrated Modeling of Optical Systems User's Manual, Release 2.0, JPL D-13040, November 15, 1995

[4] Geary J. M., Introduction to Wavefront Sensors, SPIE Press Vol. TT18, 1995

[5] Melody J. W., Discrete Frequency and Broadband Reaction Wheel Disturbance Models, JPL Interoffice Memorandum 3411-95-200csi , June 1, 1995

[6] URL Source: http://www.ithaco.com/, Ithaco E-Type Reaction Wheel product specification